Strain- and temperature-induced polymorphism of poly(dimethylsiloxane)

Masatoshi Tosaka,[†] Miki Noda,[‡] Kazuta Ito,[‡] Kazunobu Senoo,[‡] Koki Aoyama,[§] and Noboru Ohta[§]*

[†] Institute for Chemical Research, Kyoto University, Gokasho, Uji, Kyoto-fu 611-0011, Japan

[‡] Sumitomo Bakelite Co. Ltd., 1-1-5 Murotani, Nishi-ku, Kobe, Hyogo 651-2241, Japan

[§] SPring-8 / JASRI, 1-1-1 Kouto, Sayo-cho, Sayo-gun, Hyogo 679-5198, Japan

* Corresponding Author

E-mail: tosaka@scl.kyoto-u.ac.jp, Tel: +81-774-38-3062, Fax: +81-774-38-3067

ELECTRONIC SUPPLEMENTARY MATERIAL: The online version of this article contains supplementary materials, which are available to authorized users.

KEYWORDS: Strain-induced crystallization, conformation, wide-angle X-ray diffraction, network polymer, skeletal structure, silicone rubber

ABSTRACT: Phase behavior of silica-filled poly(dimethylsiloxane) (PDMS) network was investigated by wide-angle X-ray diffraction (WAXD) under various strain ratio between room temperature and -100°C, and anomalous polymorphic behavior was discovered. At room temperature, when sufficient strain was applied, PDMS network was found to transform into the mesomorphic phase from which only a pair of sharp equatorial reflections and faint meridional scattering were obtained in the WAXD pattern. At low temperature, PDMS network crystallized into one of three different crystal forms according to strain ratio. These crystal forms were denoted as α, transient and β forms in the descending order of corresponding strain ratio. The mesomorphic phase at room temperature transformed into the crystalline α form by reducing temperature. There was an anomalous feature about the transition of the crystalline forms that the position of reflections in the WAXD pattern changed continuously and reversibly with strain between the α and the β forms through the transient form, while keeping the diffraction angles almost unchanged.

INTRODUCTION

Poly(dimethylsiloxane) (PDMS) is the most widely used silicon-based organic polymer. Especially in many different medical applications, PDMS is irreplaceable because of the physiological inertness and the non-toxic nature. Its unique characteristics originate from the main-chain structure. The very open Si-O-Si bond angle and the large interatomic distance results in very low (practically zero) rotational energy for Si-O, and accordingly, the molecular chains of PDMS are exceptionally flexible [1]. In contrast to the carbon-skeletal polymer whose molecular chains in the crystal are mostly constrained to adopt the trans (T), gauche (G) or skew (S) conformations due to the rotational potential barrier, molecular chains of PDMS in the crystal phase should be able to exhibit higher degree of freedom. However, such a consideration has not been reflected in the previous studies on the crystal structure of PDMS.

Crystal structure of PDMS was analyzed by Damaschun [2] in 1962 using silica-filled samples under relatively large deformation at -90°C. In this work, the crystal unit cell was proposed to be monoclinic with a = 1.3 nm, b (fiber axis) = 0.83 nm, c = 0.775 nm, and β = 60°. A twofold helical conformation of the polymer chain with six monomers per turn was suggested. This crystal structure had been admitted without further investigation by wide-angle x-ray diffraction (WAXD), though the numerical information about the reflection intensities and the atomic coordinates have not been presented. In 1991, Schilling et al. [3] studied PDMS crystals by ^{29}Si and ^{13}C NMR spectroscopy. They mentioned that the results of this NMR study were inconsistent with the Damaschun’s proposal. Instead of multiple resonances as expected from the twofold helical conformation, single resonances were observed for both nuclei. (Schilling et al. assumed the $TTS^+S^-G^+G^+$ sequence on the basis of Damaschun’s illustration. However, by constructing the three dimensional model, we found that this sequence does not result in the twofold but in the threefold helical conformation.) Later on, Albouy [4] studied weakly stretched PDMS specimens by WAXD, and claimed that Damaschun's proposal was inappropriate, suspecting qualitative modification of the texture pattern for samples submitted to high extension ratios. The unit cell suggested by Albouy was tetragonal, with a = ca. 0.83 nm and c (fiber axis) = ca. 1.2 nm. The polymer chain was supposed to adopt a fourfold helical conformation, which is more extended than the Damaschun's model. However, no numerical data about WAXD intensity and atomic coordinates were presented also by Albouy. In this way, the crystal structure of PDMS has not been studied in detail, and accordingly, the relationship between the rotational freedom around the Si-O bond and the resulted crystal structure has not been discussed.

Here, we report on discovery of polymorphic behavior in crosslinked PDMS, which depends on strain and temperature. Even at room temperature, stretched PDMS network was found to transform into mesomorphic phase. At low temperature, existence of multiple crystal forms and continuous structure transition between them was also discovered. Because such continuity is anomalous for crystal transformation, the specific conformational freedom of the siloxane skeletal should be considered.

EXPERIMENTAL SECTION

Materials

Sheets of silica-filled PDMS samples (ca. 1 mm thick) were prepared as follows. End-linked PDMS was prepared by heating (70 °C, 24h) the mixture of 25wt% of vinyl-terminated PDMS (Mw = 43,000), 75wt% of vinyl-terminated PDMS with silica filler (Mw = 28,000, silica 15～

18%), 0.6 equiv. (relative to the vinyl groups) of tetrakis(dimethylsiloxy)silane (crosslinking agent) and chloroplatinic acid (0.1 mol/l isopropanol solution, catalyst).

Randomly crosslinked PDMS was prepared by heating (pre-baking at 170 °C, 10 min and subsequently at 200 °C , 4 h) the ingredients according to the recipe in Table 1.

WAXD and simultaneous tensile measurements

Both the synchrotron beam source and a conventional X-ray instrument were used for the WAXD analysis. The former is mainly used for the WAXD analysis at room temperature, and the latter was used for the temperature-controlled measurements. In both cases, a tensile machine was placed on the path of X-ray. Two-dimensional WAXD patterns and the tensile force were recorded simultaneously.

The synchrotron experiments were performed at BL-40XU beam line in SPring-8, Japan. The wave length was 0.0832 nm (15 keV). Ring-shaped specimens for our original tensile machine [5] were die-cut from the sample sheets. The width and circumference of the specimens were ca. 1 mm and 50 mm, respectively. The WAXD patterns were recorded using a CCD camera. The camera length was ca. 180 mm.

For the temperature-controlled WAXD measurement, a conventional X-ray instrument (Rigaku Nano-Viewer, CuKa radiation monochromatized with a confocal mirror, 40 kV/30 mA) was used. The wave length was 0.154 nm. Rectangular specimens (ca. 30 mm × 5 mm) were cut out from the sample sheets. The specimen was stretched and cooled in nitrogen atmosphere using a Linkam TST350 tensile testing stage. The WAXD patterns were recorded using a two-dimensional photon counting detector (PILATUS100K/R) or an imaging plate (IP). The camera length was ca. 100 mm (for PILATUS) or ca. 80 mm (for IP).

RESULTS AND DUSCUSSION

Mesomorphic phase

At room temperature, the undeformed specimens presented isotropic amorphous halo from unoriented PDMS molecules in the WAXD pattern. When the specimens were subjected to uniaxial stretching, a pair of sharp reflections appeared on the equator near the amorphous halo, as shown in Fig. 1a. For detailed investigation of this feature, equatorial intensity profiles (Fig. 1b) were analyzed. With the increase in strain ratio (*SR*), the maximum of the intensity shifted to the higher q (Fig. 1c), and at the same time, the intensity profile became sharper. This peak shift is attributed to the development of the new reflections which are overlapping the amorphous halo. As shown in Fig. 1c, we observed a certain strain ratio for the onset of the peak shift, namely, the emergence of the new reflections. Accordingly, the peak shift should indicate a kind of structure transition which occurs above a certain strain. This phenomenon was found in all the PDMS samples, though the degree of peak shift and its onset strain changed with the formulation and crosslinking density of the samples. Other researchers also reported the emergence of the sharp reflections in oriented PDMS at room temperature [6,7], indicating that this phenomenon is universal for the PDMS networks. In the previous studies, these sharp reflections were attributed to the oriented amorphous [6] or the crystal phase [7]. However, we will present shortly that these attributions should be reconsidered.

There is another feature in the WAXD pattern of the highly-stretched specimens. Along with the above-mentioned sharp reflections on the equator, faint scattering on the meridian was sometimes observed. The scattering in question is indicated by arrows in Fig. 1a. The same feature of the WAXD pattern is found in the work by Ohlberg et al. [6]

It is a natural consequence to guess that these features in the WAXD pattern could be related to strain-induced crystallization [8-10]. Though melting temperature (T_m) of PDMS is far below room temperature (e.g., below -30°C, according to our preliminary DSC experiment), T_m of polymer network is considerably elevated by the application of strain [10-13]. Delides and Shepherd [7] indeed regarded the sharp Debye-Scherrer ring in the radiation crosslinked sample as a result of strain-induced crystallization at room temperature. For the confirmation of this interpretation, highly stretched PDMS specimens that showed the sharp equatorial reflections (Fig. 1a) were slowly cooled down. The final WAXD pattern at -100 °C is shown in Fig. 2a, in which the sharp equatorial reflections are also observed. We examined the WAXD patterns during the cooling process (from Fig. 1a to Fig. 2a) and found the emergence of sharp reflections of the "real" crystal phase at certain low temperature. In order to demonstrate this "real" crystallization, the equatorial intensity profiles during the cooling process (Fig. 3a) were separated into two components by peak fitting software [14]; one was the sharp peak which existed at room temperature, and the other was much sharper crystalline peak which appeared at low temperature. The relative area of the crystalline peak, namely crystallinity index, was estimated and plotted as a function of temperature in Fig. 3b (the detailed procedure is explained in Supplementary Material - Document). We can observe the clearly defined onset of crystallization at ca. -60 °C. In some of the samples, crystallization was also detected as an abrupt increase in tensile force (Supplementary Material - Document). The transition into the "real" crystal phase at low temperature implies that the

WAXD pattern at room temperature (Fig. 1a) is attributed to another thermodynamic phase. The sharp equatorial reflections indicate regularity of molecular chains packing, and at the same time, the faint scattering on the meridian suggests weak helical periodicity. Such a less ordered structure than crystal is attributed to the mesomorphic phase. The Debye-Scherrer ring observed by Delides and Shepherd [7] must be also attributed to the mesomorphic phase.

Crystal polymorphism

We realized that the WAXD pattern of highly strained PDMS at -100°C (Fig. 2a) corresponds to the one reported by Damaschun [2]. This early work was proved to be based on reliable experimental results which were reproduced by other researchers (including Ref. [6]). In Fig. 2a, weak reflections which have not been recognized before [2] (e.g., 200 reflection) can be observed. Using the twelve independent reflections, the lattice constants of the monoclinic unit cell were tentatively refined (Supplementary Material - Document) because the 422 reflection could not be explained by the lattice constants in the previous work [2]. The unit cell parameters estimated from the WAXD pattern in Fig. 2a were a = 1.439 nm, b (fiber axis) = 0.840 nm, c = 0.854 nm, and β = 55.6°.

Meanwhile, when the applied strain was small, PDMS samples were found to present the alternative WAXD pattern at low temperature, that has been reported by Albouy [4] (Fig. 2c). Polymorphism of PDMS crystal has not been recognized before, but the above-mentioned results clearly demonstrate the existence of different crystal forms. For convenience, we refer to the former crystal form (characterized by the WAXD pattern in Fig. 2a) as the α form, and the latter (characterized by the WAXD pattern in Fig. 2c) as the β form. The same PDMS specimen crystallized in the α or in the β form according to the degree of strain; the α form is the high strain phase.

Surprisingly, when the strain ratio was intermediate value between the occurrence of the α and the β forms, the WAXD pattern was attributable to the neither form, as shown in Fig. 2b. (Ohlberg et al.[6] reported the similar WAXD pattern, not noticing the polymorphism.) That is to say, this WAXD pattern cannot be explained by simple orientational fluctuation or by superposition of the α and the β forms. We refer to the crystal structure corresponding to Fig. 2b as the transient form, because this crystal structure seems to change continuously between the α and the β forms, as mentioned below. Note that, in our experiments, *the amorphous specimen was deformed at room temperature, and directly crystallized into the transient form by cooling*. Accordingly, the transient form is not the result of mechanical destruction of the α or the β forms, but a stable structure at the corresponding specific strain ratio.

There is a peculiar coincidence among the WAXD patterns of these three crystalline forms. Most of the reflections (except weak ones such as 200 and 222 of the α form) appear on the same concentric circles, though the crystal structure is different. That is to say, in all the three forms, reflections appeared at q (nm^{-1}) = 9.6, 15.7, 18.3, and so on. Furthermore, the relative relationship among integrated intensities at these q values are also almost unchanged (Fig. 1d). On the basis of these feature, the transition between the α and the β forms was traced using the azimuthal intensity distribution. The specimen was deformed at 25°C to the predetermined strain value and cooled to -100°C. From the WAXD patterns at -100°C, azimuthal intensity distributions around q = 9.6 nm^{-1} were extracted (Supplementary Material – Document). The azimuthal intensity distribution was separated into independent peaks by peak fitting software [14], and the latitude (namely, azimuthal angle from the equator) of the maximum was estimated for each of the peak.

The relationship between the peak latitudes and strain ratio for various samples is shown in Fig. 4. The β form is characterized by the two peaks at the latitude of ca. ±30°. They separated into four peaks while the transient form appeared and the peak latitudes shifted continuously and reversibly with strain ratio. At large strain, the two of four peaks near the equator merged into one and resulted in the three peaks (on the equator and at the latitude of ca. ±60°) characterizing the α form. Position of other reflections also changed continuously in the similar way with strain ratio. The strain ratios to induce this kind of transitions changed according to the composition of the sample, as shown in Fig. 4. As this observation demonstrates, the structure of the transient form changes continuously and reversibly with strain. Here, we emphasize again that the transient form cannot be explained by simple orientational fluctuation of another form. For example, on transition from Fig. 2a (α form) to Fig. 2b (transient form), the 001 reflection separates and depart from the equator, while the 111 reflection moves toward the equator. That is to say, the azimuthal directions of the movement are opposite between the 001 and 111 reflections. (An animation in mpg format demonstrating this peculiarity is available as a Supplementary Material - Movie.) Such a movement of reflections is inconsistent with the simple rotation of the fiber axis.

In general, crystalline polymorphism reflects the difference in molecular chain conformation and packing in the unit cell. Such structure transition should modify characteristic lengths (e.g., intermolecular distance, helical pitch, and so on) that are related to diffraction angle. Therefore, the continuous structure change of the PDMS crystals between the α and the β forms through the transient form, each presenting strong reflections at the same diffraction angles, is quite anomalous. We guess that this peculiar behavior may be related to the characteristic of the siloxane skeletal structure. In the case of carbon-skeletal polymer, the possible helical structures are limited to adopt the combination of T, G and S conformations. On the other hand, the rotation around the Si-O bond is practically free. As a result, the continuous structure change during the emergence of the transient form could be possible. Unfortunately, atomic coordinates in each crystal form, that are desired for the better understanding of this mystifying structure change, are still not reported. Even the models of the chain conformation that were proposed in previous studies [2,4] are questionable. If we believe the previous studies, the molecular chains in the β form have to adopt more extended conformation than in the α form, though the smaller strain is applied to the sample for the emergence of the former. Because such an inversed relationship between the macroscopic strain and the molecular conformation is unlikely, alternative helical structures may have to be taken into account. Determination of the atomic coordinates in the PDMS crystals and the analysis of the transition among them is our future task.

CONCLUSION

We found, for the first time, the polymorphic behavior of PDMS. At room temperature, when sufficient orientation is applied, PDMS transforms into the mesomorphic phase. At low temperature, PDMS network crystallized into one of the α, transient and the β forms in the descending order of corresponding strain ratio. The mesomorphic phase at room temperature transformed into the crystalline α form by reducing temperature. The position of reflections in the WAXD pattern changed continuously and reversibly with strain between the α and the β forms through the transient form, while keeping the diffraction angles almost unchanged.

ACKNOWLEDGMENT

This study was partly supported by a Grant-in Aid for Scientific Research (C), No. 20550187 from Japan Society for the Promotion of Science (to M. Tosaka). The synchrotron radiation experiments were performed at the BL40XU of SPring-8 with the approval of the Japan Synchrotron Radiation Research Institute (JASRI) (Proposal No. 2010B1215, 2012A1044, 2013A1203).

REFERENCES

1. Owen M J (1981) Why silicones behave funny. Chemtech 11: 288-292
2. Damaschun V G (1962) Röntgenographische Untersuchung der Struktur von Silikongummi. Kolloid-Z 180: 65-67
3. Schilling F C, Gomez M A, Tonelli A E (1991) Solid-state NMR observations of the crystalline conformation of poly(dimethylsi1oxane). Macromolecules 24: 6552-6553
4. Albouy P-A (2000) The conformation of poly(dimethylsiloxane) in the crystalline state. Polymer 41: 3083-3086
5. Tosaka M, Senoo K, Sato K, Noda M, Ohta N (2012) Detection of fast and slow crystallization processes in instantaneously-strained samples of cis-1,4-polyisoprene. Polymer 53: 864-872
6. Ohlberg S M, Alexanders L E, Warrick E L (1958) Crystallinity and orientation in silicone rubber. I. X-Ray studies. J Polym Sci 27: 1-17
7. Delides C G, Shepherd I W (1977) Crystallization in poly(dimethyl siloxane) networks formed by γ -irradiation. Polymer 18: 97-98
8. Murakami S, Senoo K, Toki S, Kohjiya S (2002) Structural development of natural rubber during uniaxial stretching by in situ wide angle X-ray diffraction using a synchrotron radiation. Polymer 43: 2117-2120
9. Toki S, Sics I, Ran S, Liu L, Hsiao B S, Murakami S, Senoo K, Kohjiya S (2002) New insights into structural development in natural rubber during uniaxial deformation by in situ synchrotron X-ray diffraction. Macromolecules 35: 6578-6584

10. Tosaka M, Murakami S, Poompradub S, Kohjiya S, Ikeda Y, Toki S, Sics I, Hsiao B S (2004) Orientation and crystallization of natural rubber network as revealed by WAXD using synchrotron radiation. Macromolecules 37: 3299-3309
11. Flory P J (1947) Thermodynamics of crystallization in high polymers. I. Crystallization induced by stretching. J Chem Phys 15: 397-408
12. Yamamoto M, White J L (1971) Theory of deformation and strain-induced crystallization of an elastomeric network polymer. J Polym Sci Part A-2 9: 1399-1415
13. Tosaka M (2009) A route for the thermodynamic description of strain-induced crystallization in sulfur-cured natural rubber. Macromolecules 42: 6166-6174
14. Wojdyr M (2010) Fityk: a general-purpose peak fitting program. J Appl Cryst 43: 1126-1128

Figure captions

Fig. 1 WAXD pattern of end-linked PDMS stretched to *SR* = 6 (a), equatorial intensity profiles at various *SR* (b), and peak *q* values of the equatorial intensity distribution as a function of strain ratio (c) at room temperature

Fig. 2 WAXD patterns of end-linked PDMS stretched to *SR* = 6 (a), *SR* = 2.5 (b) and *SR* = 2 (c) at -100 °C, and their one-dimensional intensity profiles by circular integration (d)

Fig. 3 Equatorial intensity profiles of randomly crosslinked PDMS 3B (a) and temperature dependence of crystallinity index during the cooling process (b)

Fig. 4 Latitude of the reflection peaks around $q = 9.6\ \mathrm{nm}^{-1}$ as a function of strain ratio for the end-linked sample (a) and randomly crosslinked samples (b-d)

Table 1 Recipe of the randomly crosslinked PDMS (in parts by weight)

Sample code	PDMS[a]	Silica filler[b]	Crosslinking agent[c]	Catalyst[d]
1B	100	60	0.23	0.05
3B	100	60	0.495	0.05
5B	100	60	0.91	0.05

[a] 0.3 mol% of methyl groups were substituted by vinyl groups

[b] average size of primary particles is 7 nm

[c] PDMS in which 0.4 mol% of methyl groups were substituted by hydrogen

[d] platinum divinyl tetramethyldisiloxane complex

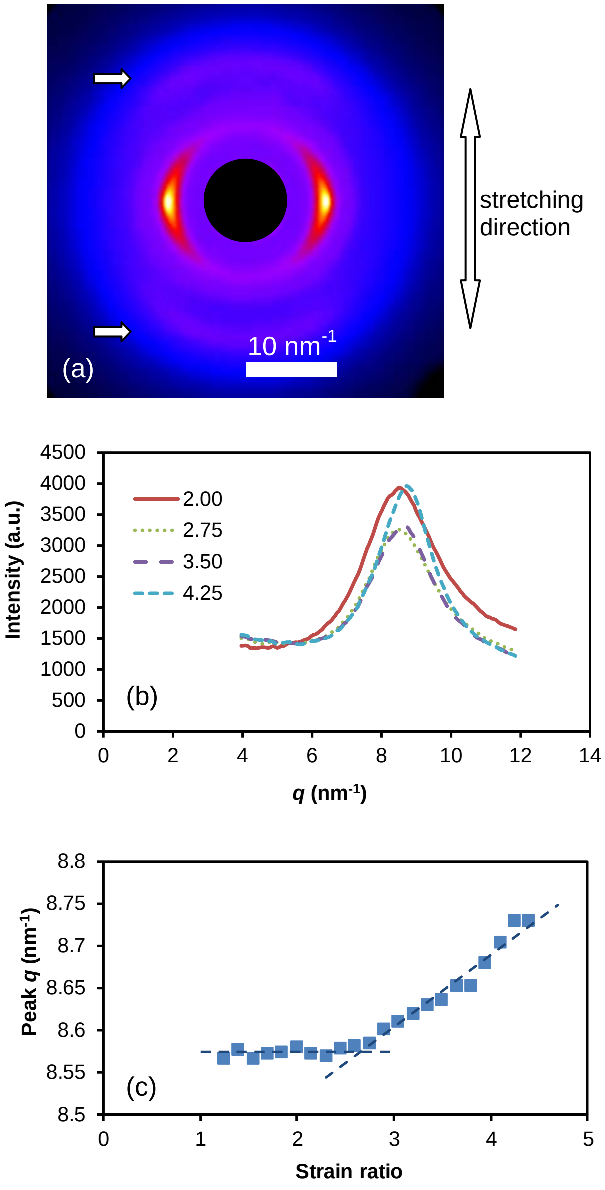
stretching direction
10 nm^{-1}
(a)
4500
4000
3500
3000
2500
2000
1500
1000
500
0
Intensity (a.u.)
2.00
2.75
3.50
4.25
(b)
0
2
4
6
8
10
12
14
q (nm^{-1})
8.8
8.75
8.7
8.65
8.6
8.55
8.5
Peak q (nm^{-1})
(c)
0
1
2
3
4
5
Strain ratio

Fig. 1

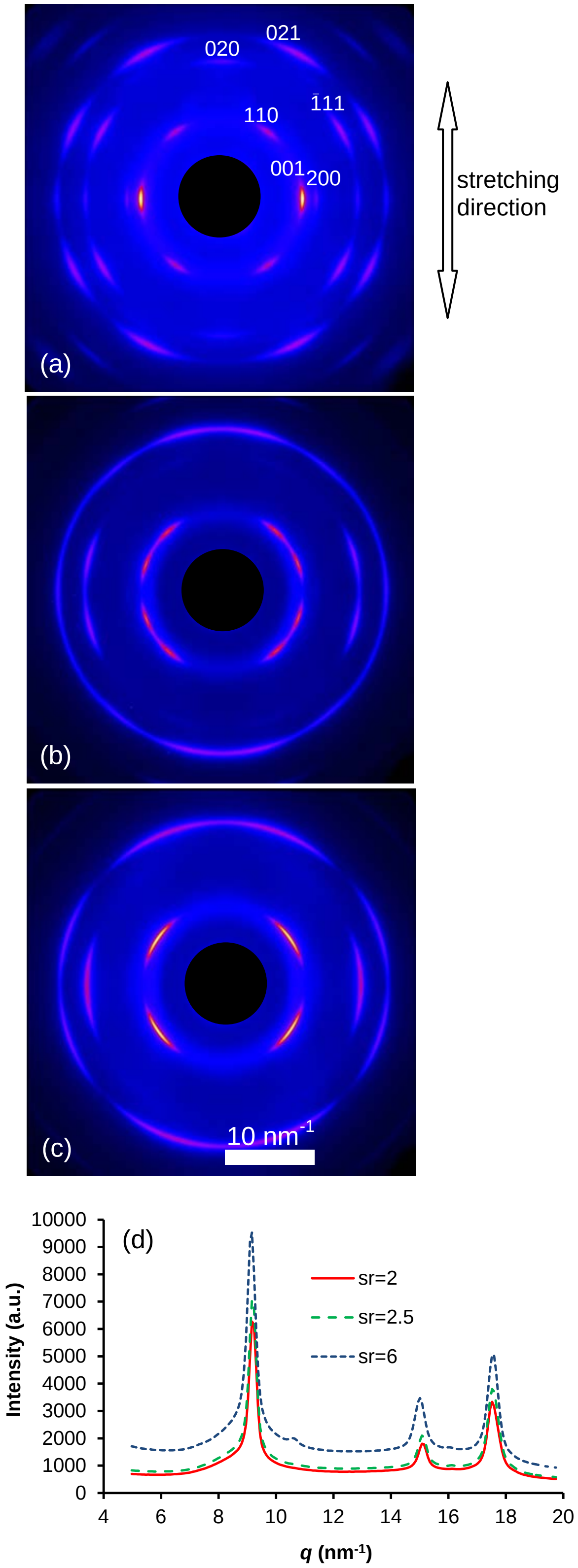
020
021
110
$\bar{1}11$
001
200
stretching direction
(a)
(b)
10 nm^{-1}
(c)
(d)
Intensity (a.u.)
10000
9000
8000
7000
6000
5000
4000
3000
2000
1000
0
sr=2
sr=2.5
sr=6
4
6
8
10
12
14
16
18
20
q (nm^{-1})

Fig. 2

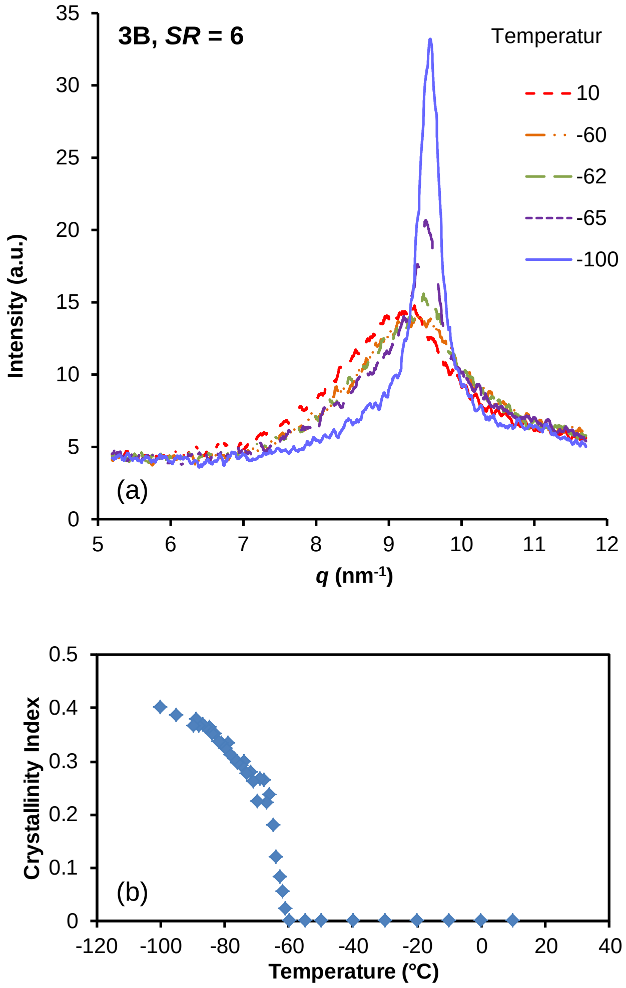
3B, *SR* = 6
Temperatur
10
-60
-62
-65
-100
Intensity (a.u.)
0
5
10
15
20
25
30
35
(a)
5
6
7
8
9
10
11
12
q (nm⁻¹)
Crystallinity Index
0
0.1
0.2
0.3
0.4
0.5
(b)
-120
-100
-80
-60
-40
-20
0
20
40
Temperature (°C)

Fig. 3

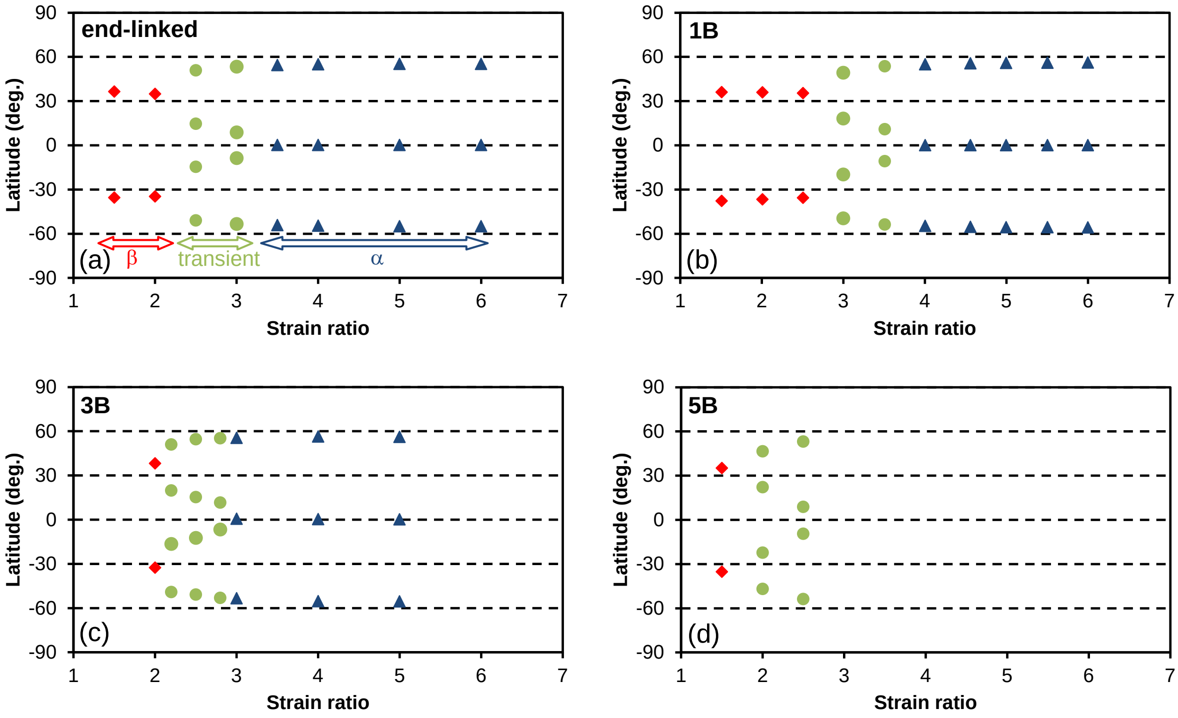
end-linked
1B
3B
5B
(a)
(b)
(c)
(d)
β
transient
α
Latitude (deg.)
Strain ratio
90
60
30
0
-30
-60
-90
1
2
3
4
5
6
7

Fig. 4